CONF-950828--25

CONVECTIVE HEAT TRANSFER BEHAVIOR OF THE PRODUCT SLURRY OF THE NITRATE TO AMMONIA AND CERAMIC (NAC) PROCESS

I. Muguercia, G. Yang, and M. A. Ebadian*
Department of Mechanical Engineering
Florida International University
Miami, FL 33199

D. D. Lee, A. J. Mattus, and R. D. Hunt
Chemical Technology Division
Oak Ridge National Laboratory
Oak Ridge, TN 37831

ABSTRACT

The Nitrate to Ammonia and Ceramic (NAC) process is an innovative technology for immobilizing liquid form low level radioactive waste (LLW). An experimental study has been conducted to measure the heat transfer properties of the NAC product slurry. The results indicate that the heat transfer coefficient for both concentration slurries is much higher than that of pure water, which may be due to the higher conductivity of the gibbsite powder. For the 20% concentration slurry, the heat transfer coefficient increased as the generalized Reynolds number and slurry temperature increased. The heat transfer coefficient of 40% is a function of the Reynolds number only. The test results also indicate that the thermal entrance region can be observed only when the generalized Reynolds number is smaller than 1,000. The correlation equation is also developed based on the experimental data in this paper.

NOMENCLATURE

A	surface area of the pipe, m^2
C_p	Heat capacity, J kg^{-1} $°C^{-1}$
d	pipe diameter, m
h	convective heat transfer coefficient, $Wm^{-2}°C^{-1}$, Eq. (1.5)
K	fluid consistency, N $sec^{3-n}m^{-2}$
k	conductivity, W(m °C)$^{-1}$
L	pipe length, m
m	mass flow rate kg/s
n	flow index
Nu	Nusselt number
Pr	Prandtl number
q	heat transfer rate, W m^{-2}
Re	Reynolds number
Re_g	generalized Reynolds number
T	temperature, °C
u_m	slurry mean velocity, m sec^{-1}

Greek Symbols

Γ	pseudo-shear rate, sec^{-1}
γ	shear rate, sec^{-1}
Δp	pressure drop along the test section $\frac{N}{m^2}$
μ_a	apparent viscosity, N sec^{2-n}
ρ	slurry density, kg m^{-3}
τ	shear stress, N m^{-2}
ϕ	solids concentration

Subscript

ℓ	liquid
m	mean
s	solid
w	wall

*ASME Fellow and corresponding author.

INTRODUCTION

Since World War II, millions of tons of liquid form low-level radioactive waste (LLW) have been generated during the production of weapons materials. The majority of the LLW has been temporarily stored in 300 underground storage tanks at five U.S. Department of Energy (DOE) sites. Radioactive waste in the liquid state poses a great threat, due to the potential for seepage into groundwater supplies, and therefore, must be immobilized before final disposal. Preliminary studies have indicated that more than 80% of the chemical concentrations in this LLW is composed of sodium nitrate. The characteristics of this sodium nitrate–based waste are as

follows: pH, either <1 or >12, with the total salt content of >5 *M*, the sodium content of >1.5 *M*, and a radiation level of 0.1 to 1.2 R/h. Recently, a new immobilization technique for the LLW, the Nitrate to Ammonia and Ceramic (NAC) process, has been developed (Mattus et al., 1993 and Mattus and Lee, 1993). Laboratory experiments have shown that a decontaminated nitrate in the LLW can be converted in to ammonia gas by adding aluminum particles. The final product of the NAC process is gibbsite, which can be further sintered to a ceramic waste form. Radioactive species, such as plutonium and strontium, will enter the solid ceramic phase during the reduction process. The alumina-based ceramic will be further calcined, pressed, and sintered to generate the solid waste form. Preliminary tests have indicated that the NAC process not only produces environmentally acceptable waste, but also reduces the volume of the final waste up to 70%, compared to the cement-based grout method. This volume reduction represents a significant reduction in cost for final land disposal.

The NAC process is an exothermic one that generates large amounts of heat during the chemical reaction. In order to maintain a desired operating temperature between 50° and 80°C inside the NAC reactor, a cooling system is required. To design a cooling system and the NAC reactor, one needs to know the rheological and thermal behaviors of the product slurry. An experimental measurement of the rheological properties of the NAC final product slurry was recently conducted (Muguercia, et al., 1995). The test results indicate that the NAC process slurry exhibits a non-Newtonian behavior at a low shear rate and becomes Newtonian fluid at a high shear rate. The transition from the non-Newtonian fluid to the Newtonian fluid coincides with the transition from laminar flow to turbulent flow—that is, the transition occurs at the generalized Reynolds number of around 2,600. In the non-Newtonian fluid region, the slurry acts as pseudo-plastic fluid when the solid concentration is higher than 30%, and delatant fluid when the solid concentration is below 25%. The objective of this study is to experimentally determine the heat transfer behavior of the final product slurry.

THE TEST APPARATUS

A test apparatus has been designed and constructed to measure the heat transfer coefficient of the pipe flow. Figure 1 illustrates the test facility, which consists of the NAC process reactor, the test loop, and the associated instrumentation. The NAC reactor is a 6-liter chemical reactor (model BioFlo IIC manufactured by New Brunswick Scientific), which automatically mixes the slurry and controls the slurry temperature. The gibbsite slurry is pumped from the reactor to a test loop and then discharged back to the reactor. The test loop is constructed of a 2.18cm ID stainless steel pipe and has two test sections: the heating temperature control sections. The 2.44 m (8 ft) heating section is used to measure the heat transfer coefficient of the slurry pipe flow. The direct current heating technique was employed by passing high current DC through the test section. The current source was a constant-voltage/constant-current DC arc welder. The capacity of the heating source is 3.5 kW. The non-uniformity in the heat flux, due to resisting change of the stainless pipe, was less than 3%. The test section is insulated with fiberglass packing. The 2.44 m (8 ft) temperature control section is a double-pipe heat exchanger, which is used to provide the additional temperature control for the slurry inside the reactor.

The slurry flow rate is measured by a magnetic flowmeter (Endress & Houser, Inc.) with an uncertainty of less than ±1%. Two thermocouples were used to measure the slurry temperatures at both the inlet and outlet of the test section. Another 40 thermocouples were installed along the test section to determine the temperature of the pipe wall. Before installation, all thermocouples were calibrated with a precision thermometer and have an accuracy of ±0.1 °C. After installing all the thermocouples, the thermocouples were calibrated again in situ at three fixed temperatures. The reading differences of all thermocouples were less than ±0.2 °C. All thermocouples were connected to a Hewlett-Packard data acquisition system, and the temperatures were automatically recorded by a computer. The overall uncertainty of the temperature measurement was ±0.3 °C. During the test, the temperature drop of the slurry was usually less than 5°C, therefore, the change of the physical properties of the slurry can be neglected. The FE-125 magnetic flowmeter was used to measure the slurry flow rate through the pipe. The uncertainty of the flow measurement is ±2 %. The uncertainties of the generalized Reynolds number and the Nusselt number are 3.5 % and 8.9%, respectively (Figliola and Beasley, 1991).

DATA REDUCTION METHODOLOGY

The slurry flow rate, temperature, and pressure difference of the test section were continuously recorded during the test. The generalized Reynolds number can be calculated by the following equation:

$$Re_g = (\rho\, u_m^{2-n}\, d^n)/(K * 8^{n-1}) , \quad (1)$$

where ρ and u_m are the density and the mean flow velocity of the slurry. d is the diameter of the pipe and n and K are the flow index and fluid consistency, respectively. The n and K are physical properties of the slurry, which can be found by plotting the shear stress, τ, and pseudo-shear rate, Γ, relation in a logarithmic domain (Irvine and Karni, 1987, and Wasp et. al. 1977). The τ and Γ are defined by:

$$\tau = d\Delta p/(4L) , \quad (2)$$

$$\Gamma = 8\, u_m/d, \quad (3)$$

where L is the distance between the two pressure transducers, and Δp is the corresponding pressure drop. The shear rate and apparent viscosity can then be calculated by:

$$\gamma = (3n+1)/4\ \Gamma, \tag{4}$$

$$\mu_a = \tau \gamma^{-1} = K \gamma^{n-1}. \tag{5}$$

The Nusselt number is defined by:

$$Nu = h\ d/k, \tag{6}$$

where h and k are the convective heat transfer coefficient and conductivity coefficient, respectively. The conductivity coefficient for the slurry can be found if the solids concentration and the conductivity coefficients are known for both the solids and the liquid (Wasp et al., 1977):

$$k_m = k_\ell \left[\frac{2k_\ell + k_s - 2\phi(k_\ell - k_s)}{2k_\ell + k_s + \phi(k_\ell - k_s)} \right], \tag{7}$$

where the subscripts, ℓ and s, indicate the liquid and solid phase, respectively, and ϕ is the solids concentration. The convective heat transfer coefficient, h, is found by:

$$h = q/\{A(T_w - T_m)\}, \tag{8}$$

where A is the surface area of the pipe, and T_w and T_m are the measured temperatures of the wall and the slurry, respectively. The heat transfer rate, q, was calculated in two ways. One through the electrical energy consumed by the electric heaters, and the other calculated by:

$$q = m\ C_p\ (T_{m2} - T_{m1}), \tag{9}$$

where m is the mass flow rate of the slurry, and T_{m2} and T_{m1} are the slurry temperatures in the outlet and the inlet, respectively.

RESULTS AND DISCUSSION

Rheology Behavior of the Product Slurry

The rheological behavior of the product slurry was recently experimentally measured (Muguercia et al., 1995). The test was conducted on a 2.18 cm ID test loop. The slurry flow rate varied between 5 and 37 *l*/min, which corresponds to the velocities of between 0.25 - 1.75 m/sec. The major results can be summarized as:

i. The rheological behavior of the slurry is strongly dependent on the solids concentration. At a low concentration, as seen in Fig. 2, the slurry with 20% solids concentration exhibits a dilatant fluid behavior, while the 40% concentration slurry behaves as a pseudo-plastic fluid. The transition from a dilatant fluid to a pseudo-plastic fluid occurs between a 25% to 30% solids concentration.

ii. The slurry with a concentration between 17% to 23% solids concentration has a very similar rheological behavior, and seems to be insensitive to the change of the slurry temperature. The constitutive relation can be written as:

$$\tau = kg^{n-1} = 4.083 \times 10^{-4}\ \gamma^{1.566}\ [N/m^2]. \tag{10}$$

iii. The slurry with a concentration between 33% and 40% solids concentration exhibits a very similar rheological behavior. In the laminar flow regions (low shear rate), the slurry behaves as a pseudo-plastic non-Newtonian fluid and changes to a Newtonian fluid in the turbulent region (or high shear rate region). In the non-Newtonian flow region, the constitutive relation for the slurry at 65°C can be written as:

$$\tau = 2.079\gamma^{0.219}. \tag{11}$$

Unlike the low concentration slurry, the rheological behavior of the high concentration slurry is temperature dependent. The shear stress is about 10% higher than that predicted by Eq. (11) at a temperature of 80°C, and 10% lower at 50°C.

It needs to be mentioned that due to the different fluid index, the 40% concentration slurry has a greater range of Generalized Reynolds number than the 20% concentration slurry with the same velocity ranges in Fig. 2.

Physical Properties of the Slurry

Non-radioactive gibbsite slurry, chemically and physically (powder size distribution) similar to the final product of the NAC process, was used to simulate the actual product slurry. The chemical compositions and the particle size distributions of the dried slurry powder are listed in Tables I and II, respectively.

Calibration of the Test Loop

Water was tested first to ensure that the thermocouples, electric heater, and insulation were in good condition. Table III shows the test results compared with the predicted results by a well known correlation equation [Incropera and DeWitt, 1990]:

$$Nu = 0.023 * Re^{4/5} Pr^{1/3}. \tag{12}$$

During the test, the water inlet temperature was controlled at 50°C. Previous research has indicated that the thermal entrance region is usually less than 20 times the pipe diameter in turbulent flow. Therefore, the entrance effect for water flow can be neglected since the entrance region is less than 10% in our test loop. Table III indicates that our test data were slightly less than the prediction; the deviation was around 6% at a small flow rate and less than 2% at a large flow rate. The test results indicate that the test facility and the instrumentation were in good condition.

TABLE 1 COMPOSITION OF THE DRIED SLURRY

Composition	Wt. %
Al_2O_3	65.1
H_2O	34.4
Soluble sodium nitrate	0.05
SiO_2	0.03
Fe_2O_3	0.008
V_2O_2	0.002
Cu	0.001
Mn	0.0015

TABLE 2 SIZE DISTRIBUTIONS OF THE DRIED SLURRY POWDER

Flow rate [l/min]	Re	Tested Nu	Predicted Nu	Deviation %
9.9	19240	93.9	100	6.1
18.2	35370	149.4	158.5	5.7
34.7	67418	261.5	265.5	1.5

Temperature Distribution

A study of the temperature distribution and heat transfer coefficient along the test section of the test loop was conducted. The slurries with a solids concentration of 20% and 40% were tested. During the test, the inlet temperature of the slurry varied from 50°C to 80°C. The volume flow rate was changed from 7 *l*/min to 35 *l*/min. which corresponded to the average velocity varying from 0.3 to 1.8 m/sec. The heating power was kept near 3kW during the test. Table IV lists the test conditions for each case.

Figure 3 illustrates the temperature distribution along the test section of the pipe for the slurry flow with a 20% solids concentration. Two cases, Re_g=2280 and Re_g=1560, corresponding to the highest (35 liter/min) and lowest slurry flow (9 liter/min) rates in the test, are presented in this figure. The solid lines indicate the slurry bulk temperature, while the open squares and dark squares indicate the wall temperature. The results show that the wall temperature is

TABLE 3 COMPARISON OF THE NUSSELT NUMBERS

Larger than 15 μm	10%
Between 7 and 15 μm	40%
Between 3 and 7 μm	40%
Smaller than 3 μm	10%

almost parallel to the slurry bulk temperature, with no obvious entrance region in this Reynolds number range. In fact, the pump was more than 6 meters away from the test section, which can ensure that the fluid reached a hydraulically full development before reaching the test section. Figure 4 shows the temperature distribution along the test section of the pipe for the case of 40% solids concentration slurry. At a greater flow rate (35 liter/min), the flow is in the turbulent (Re_g = 2720) region, and no entrance region can be observed. However, at a low flow rate, Re_g = 270, the temperature difference between the wall and the bulk temperature of the slurry is significantly increased along the test section.

Local and Average Heat Transfer Coefficients

Figure 5 illustrates the local heat transfer coefficient along the test section for the 20% concentration slurry. The test data indicates that the heat transfer coefficient is a constant along the test section at each flow rate and the slurry inlet temperature. The figure also indicates that the heat transfer rate is sensitive to both the slurry temperature and the Reynolds number. Figure 6 shows the average heat transfer coefficient changes with the generalized Reynolds number for the 20% concentration slurry. The figure indicates that the heat transfer rate of the slurry is very sensitive to the changes of the slurry temperature. Generally speaking, the heat transfer rate increased as the slurry temperature increased. The heat transfer rate will be increased nearly 10% as the temperature increases 15°C. The test data can be correlated by:

$$h = 4.04 \times 10^{-3} Re_g - 4.58 + 4.35 (T-65) Re_g^{1.16} / 10^6 .$$

In the equation T is in °C and, h is in kW/m^2 °C. The test results indicate that the heat transfer coefficient is much higher than that for pure water, which may be due to the high conductivity of the gibbsite powder. The conductivity of the gibbsite is around 3.45 - 5.18 [W/(mK)], which is 50 to 80 times higher than that of pure water.

Figure 7 shows that the local heat transfer coefficient varied along the test section. At a higher Re_g, the heat transfer exhibits a turbulent heat transfer behavior, and no obvious entrance region is observed. At a low generalized Reynolds number, a laminar entrance region can be clearly observed.

TABLE 4 TEST CONDITIONS FOR THE HEAT TRANSFER MEASUREMENT

Case	Gibbsite concentration %	Slurry inlet temperature °C	Slurry flow rate liters/min
1	20	50	9.5
2	20	50	18.2
3	20	50	22.7
4	20	65	9.5
5	20	65	18.2
6	20	65	22.7
7	20	80	9.5
8	20	80	18.2
9	20	80	22.7
10	40	50	9.4
11	40	50	18.6
12	40	50	23.5
13	40	50	34.4
14	40	65	9.4
15	40	65	18.6
16	40	65	23.5
17	40	65	34.4
18	40	80	9.4
19	40	80	18.6
20	40	80	23.5
21	40	80	34.4

The entrance region becomes short as the generalized Reynolds number increases. Figure 8 illustrates that the average heat transfer coefficient varies with the generalized Reynolds number. The figure indicates that the heat transfer coefficient increases with the generalized Reynolds number and seems insensitive to the change of the slurry temperature.

The data are correlated by:

$$h = 4.24 \times 10^{-7} \, Re_g^{1.7} + 0.768 .$$

Since the test data are in both the laminar and transition regions, the correlation curve is plotted in a solid line in the laminar region and in a dashed line in the transition region. Compared with the data in Fig. 6, this figure indicates that the heat transfer coefficient of the high concentration slurry is lower than that of the low concentration slurry.

CONCLUSION

An experimental study has been conducted to measure the heat transfer properties of the NAC product slurry. The test results indicate that the heat transfer coefficient changes with both the generalized Reynolds number and the slurry temperature for the 20% solids concentration slurry, and is a function of the generalized Reynolds number for the 40% concentration slurry. This behavior differs and originates from their rheological behavior in that the 20% concentration slurry is a dilatant fluid, while the 40% concentration slurry is a pseudo-plastic fluid. The test results indicate that the thermal entrance region can be observed only when the generalized Reynolds number is smaller than 1,000. The 20% concentration slurry has a higher heat transfer coefficient compared with that of the high concentration slurry at the same generalized Reynolds number. The results also indicate that the heat transfer coefficient for both concentration slurries is much higher than that of pure water, which may be due to the higher conductivity of the gibbsite powder.

ACKNOWLEDGMENT

The results presented in this paper were obtained in the course of research sponsored by the Department of Energy's *Office of Technology Development* under Grant No. 19X-SN855C.

REFERENCES

Mattus, A. J., Lee, D. D., Dillon, T. A., Youngblood, E. L., Tiegs, T., and Farr, L. L., 1993, "A Low Temperature Process for the Denitration of the Hanford Single Shell Tank, Nitrate-Based Waste Utilizing the Nitrate to Ammonia and Ceramic (NAC) Process, Phase II Report," a report to the U. S. Department of Energy, DE-AC05-840R21400, Oak Ridge National Laboratory.

Mattus, A. J. and Lee, D. D., 1993, "The Nitrate to Ammonia and Ceramic (NAC) Process-A Newly Developed Low Temperature Technology," Second International Mixed Waste Symposium, Aug. 17-20, 1993, Baltimore, Maryland.

Wasp, E. J., Kenny, J. P., and Gandhi, R. L., 1977 *Solid-Liquid Flow Slurry Pipeline Transportation*, Trans Tech Publications, Clausthal, Germany.

Incropera, F. P. and DeWitt, D. P., 1990, *Introduction to Heat Transfer*, 2nd Ed., Chapter 8, John Wiley & Sons, New York.

Lima, G. G. C., Navarro, R. F., de Alsina, O. L. S., "Influence of the Concentration on the Power Law Index of Alumina Suspensions in High Viscosity Newtonian Fluids," *Proceedings of the 7th International Symposium on Transport Phenomena in Manufacturing Processes*, Acapulco, Mexico, August, 1994.

Muguercia, I., Yang, G., Ebadian, M. A., Lee, D. D., Mattus, A. J., Hunt, R. D., 1995, "Rheological Properties of the Product Slurry of the Nitrate to Ammonia and Ceramic (NAC) Process," to be presented at the 1995 National Heat Transfer Conference, Portland, Oregon.

Figliola, R. S. and Beasley, D. E., 1991, *Theory and Design for Mechanical Measurements*, Chapter 5, John Wiley & Son, New York.

Irvine, T. F. and Karni, J., 1987, "Non-Newtonian Fluid Flow and Heat Transfer," Chapter 20 of the *Handbook of Single Phase Convective Heat Transfer*, ed. by S. Kakac, R. K. Shah, and W. Aung, Wiley Interscience, New York.

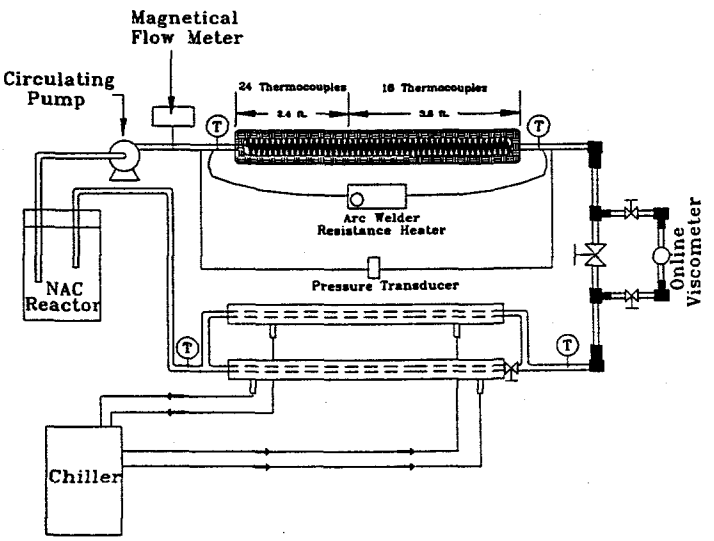

Fig. 1 Schematic of the test loop.

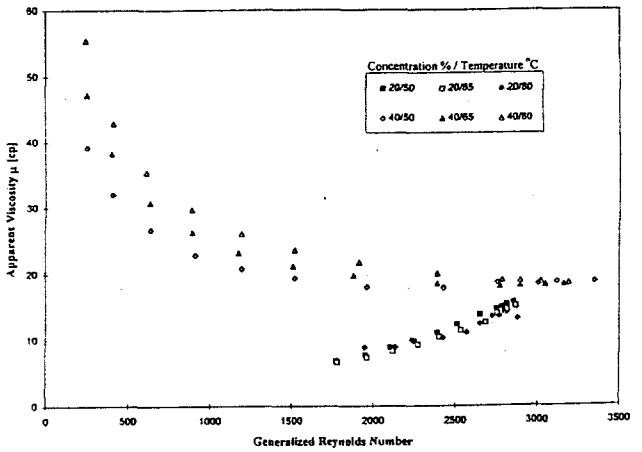

Fig. 2 Apparent viscosity as a function of the generalized Reynolds number for NCA product slurry.

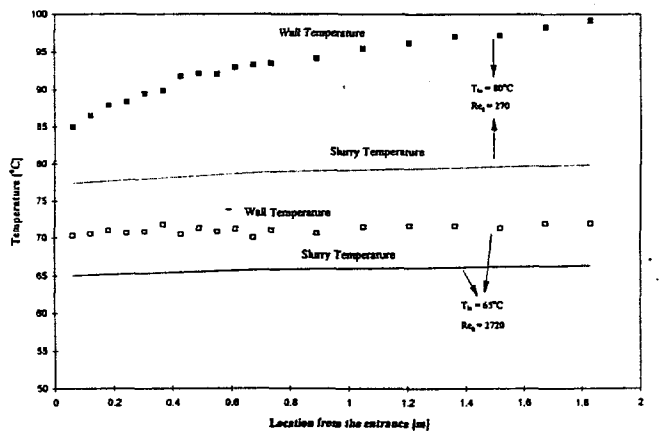

Fig. 3 Temperature distribution along the test section for 20% concentration slurry.

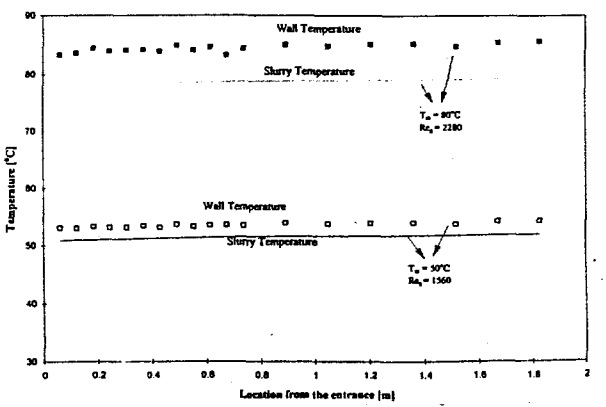

Fig. 4 Temperature distribution along the test section for 40% concentration slurry.

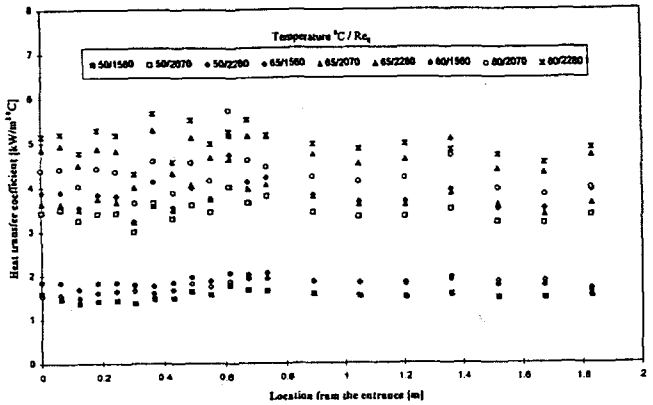

Fig. 5 Local Heat Transfer coefficient along the test section for 20% concentration slurry.

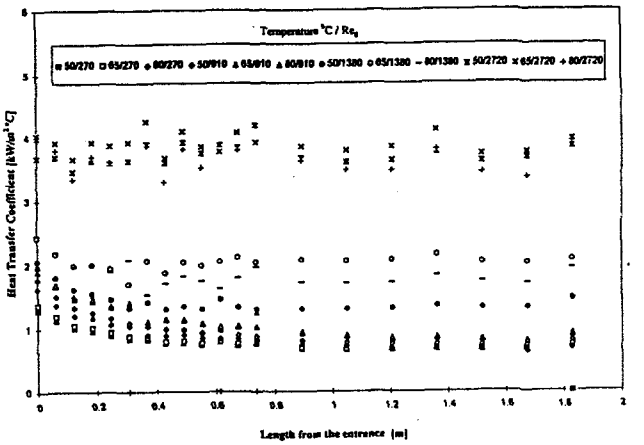

Fig. 7 Local Heat Transfer coefficient along the test section for 40% concentration slurry.

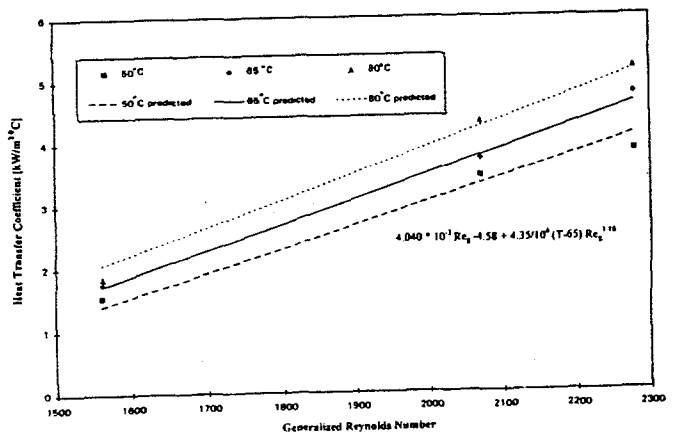

Fig. 6 Heat transfer coefficient varies with the generalized Reynolds number for 20% concentration slurry.

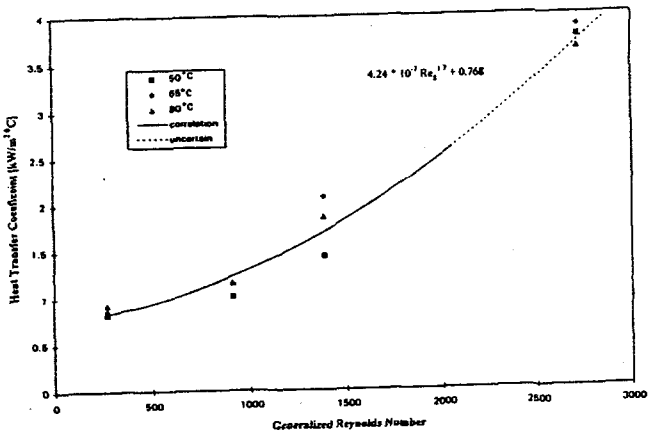

Fig. 8 Heat Transfer coefficient varies with the generalized Reynolds number of 40% of concentration slurry.

DISCLAIMER